Journal of Engineering Science and Technology Review 17 (5) (2024) 153-162

Research Article

JOURNAL OF
Engineering Science and Technology Review

www.jestr.org

A Novel Method for Microbial Detection in Wastewater Treatment

Xin Zheng[1], Chengyu Tang[1], Junrui Lv[2] and Xuegang Luo[2,*]

[1] *School of Artificial Intelligence and Bigdata, Sichuan University of Arts and Science, DaZhou 635000, China*
[2] *School of Mathematics and Computer Science, Panzhihua University, Panzhihua 617000, China*

Received 16 April 2024; Accepted 17 October 2024

Abstract

In sewage disposal processes, real-time and accurate monitoring of activated sludge microorganism types and quantities can facilitate prompt adjustments to process parameters, thereby mitigating lag effects inherent in sewage treatments. Traditionally, microscopic examinations of activated sludge microorganisms have relied on manual observation and counting by personnel to assess microorganism types and quantities under varying operational conditions. This method is inefficient and produces results lacking accuracy and consistency. To address the challenges associated with activated sludge microorganism detection, an intelligent analysis method underpinned by deep learning technology was proposed in this study. The methodology encompassed three primary stages: pre-processing of activated sludge microorganism micrographs, feature extraction from image blocks using a dedicated module, and determination of microorganism types and locations via a microbial information analysis module. To support this study, an activated sludge microorganism image dataset was constructed, comprising 2,000 images of four microorganism species: *Epistylis*, *Nematoda*, *Lecane*, and *Arcella*. Experimental results demonstrate that, the proposed method achives a mean absolute error of 5.86 and a mean squared error of 12.43 on the test set, surpassing the performance of six existing comparison methods. This exceptional performance underscores the method's significant potential for application in activated sludge microorganism detection. This study marks a substantial advancement over conventional manual detection techniques by leveraging deep learning to accurately identify activated sludge microorganisms. The proposed method enhances the speed, accuracy, and consistency of microorganism detection, thereby contributing to increased automation in water quality monitoring during sewage treatment. Ultimately, this study promotes intelligent efficiency in sewage treatments and provides a strong foundation for developing practical activated sludge microorganism detection system.

Keywords: Sewage disposal, Activated sludge microorganisms, Micrograph, Deep convolution network, Intelligent detection

1. Introduction

The global scale of urban sewage treatment is substantial, with approximately 70% of constructed sewage treatment plants applying the activated sludge method [1-2]. Currently, microscopic examination of activated sludge microorganisms relies on manual observation and counting by personnel to assess microorganism types and quantities under varying operational conditions [3]. However, this method presents significant limitations. The accuracy of microscopic observations is heavily influenced by the observer's experience and attention, leading to inconsistent and unreliable detection results across different individuals [4]. Furthermore, even experienced analysts struggle in identifying diverse microorganisms without consulting reference materials [5].

Activated sludge comprises flocculent particles formed by a complex mixture of microorganisms, including protozoa, metazoans, fungi, and bacteria, as well as suspended solids and colloidal substances in sewage. The biological constituents of activated sludge exhibit dynamic characteristics [6-7]. Understanding the fundamental relationship between the types and quantities of activated sludge microorganisms and the aquatic biochemical environment enables the assessment of sewage treatment plant operations and purification degreed by observing microbial composition under varying operational conditions [8]. In the sewage treatment process, operational anomalies often manifest with subtle changes in water quality indicators, hindering timely detection. Consequently, when sewage treatment efficiency declines and operational parameters are adjusted, the restoration of optimal activated sludge conditions can be protracted [9]. However, activated sludge microorganisms are sensitive to environmental fluctuations, resulting in pronounced shifts in microbial population and abundance under adverse conditions. Therefore, real-time and accurate monitoring of activated sludge microorganism composition is essential for efficient sewage treatment operations. This approach enables prompt adjustments to process parameters, mitigating the lag effects inherent in the treatment process [10-11]. Currently, the prevalent method of manual microscopic examination of activated sludge microorganisms cannot effectively achieve real-time, accurate monitoring, thereby contributing to lag effects within the sewage treatment process.

In recent years, deep learning methodologies, exemplified by convolutional neural networks, have catalyzed the rapid advancement of artificial intelligence (AI) [12-13]. This condition yields groundbreaking achievements in domains, such as autonomous driving [14-15], intelligent monitoring systems [16-17], and computer-aided diagnosis [18-19]. However, mature AI-based products for detecting water quality indicator microorganisms in activated sludge are currently unavailable. Moreover, research on the classification and identification of microorganisms in microscopic examinations of activated sludge remains limited.

*E-mail address: lxg_123@foxmail.com
ISSN: 1791-2377
doi:10.25103/jestr.175.20

Nevertheless, investigations in related areas suggest the feasibility of intelligent microorganism detection in activated sludge [20-21]. We introduce a novel AI method based on deep learning for activated sludge microorganism detection to address the challenges of low efficiency, poor accuracy, low consistency, and high costs associated with detecting water quality indicator microorganisms in the sewage treatment process. Our experimental findings demonstrate that the proposed method yield satisfactory detection results for micrographs of activated sludge microorganisms, exhibiting robust detection performance and generalization capabilities across various microorganisms. This approach outperforms existing methods, exhibiting significant potential for application in microscopic examinations of activated sludge microorganisms. The approach involving the integration of deep learning into the realm of microscopic examination of activated sludge microorganisms surpasses traditional manual detection methods. This technique enables the rapid identification of indicator microorganisms reflective of water quality status, including their presence, absence, and fluctuations, thereby enhancing the automation of water quality detection and improving sewage treatment efficiency.

2. State of the art

In the sewage treatment process, real-time and accurate monitoring of activated sludge microorganism types and quantities is crucial for promptly adjusting process parameters and mitigating lag effects [10-11]. Currently, microscopic examination of activated sludge microorganisms relies on manual observation and counting to assess microorganism types and quantities under varying operational conditions [3-6]. However, this method is inefficient, prone to inter-observer variability, and yields inconsistent results [4-5]. The use of computer vision technology, which has rapidly progressed, to assist in the intelligent detection of activated sludge microorganisms has become an inevitable trend [12-13]. Existing literature described the extraction of activated sludge microorganism features using fully automatic and interactive algorithms, followed by classification using decision tree methods, successfully identifying microorganisms, such as *Paramecium*, *Rotifer*, *Nematoda*, *Vorticella*, *Epistylis*, and *Catenula* [22]. Other studies had developed semi-automatic image analysis programs using multivariate statistical techniques for protozoan and metazoan identification and classification [23] and proposed protozoan detection methods using the active contour model [24]. Nevertheless, traditional image detection methods based on pattern recognition were constrained by algorithm limitations, relying solely on manually selected features and exhibiting poor generalization capabilities, thereby failing to satisfy the practical demands of activated sludge microorganism detection. In recent years, the emergence of deep learning as a new-generation AI paradigm [25-27] had prompted its application in activated sludge microorganism detection. Deep learning approaches incorporating attention mechanisms and transfer learning for accurate microorganism species identification [28] had been explored, and the YOLOv3 model with attention mechanisms had been enhanced for detecting four types of activated sludge microorganisms: *Vorticella*, *Catenula*, *Lecane*, and *Arcella* [29]. In addition, hybrid neural network models had been proposed for predicting purified sewage water quality [30]. Underwater dense object recognition methods, including recognition-by-detection, recognition-by-regression, and recognition-by-density-generation algorithms, offer potential applications in activated sludge microorganism detection [31-36]. However, these methods primarily rely on direct application of classical deep learning algorithms and lack in-depth exploration tailored to sewage treatment scenarios. No mature AI-based products for detecting water quality indicator microorganisms in activated sludge are currently available. The challenges of achieving intelligent detection of activated sludge microorganisms include the following:

(1) Existing intelligent detection methods are primarily based on pattern recognition or directly use existing deep learning models, lacking in-depth research tailored to the specific scenarios of activated sludge microorganism detection.

(2) Detection methods for activated sludge microorganisms using pattern recognition algorithms require manual feature selection to construct the detection model, resulting in limited performance and significant deficiencies in generalization ability and robustness.

(3) The backgrounds of activated sludge microorganism images are complex and are easily affected by natural environmental factors, such as lighting and impurity occlusion, as well as human factors during image acquisition. Consequently, the appearance and shape of the microorganisms are modified.

(4) Image datasets matched to real-world scenarios for performance testing of activated sludge microorganism detection methods are limited, thereby hindering research on intelligent detection methods for activated sludge microorganisms.

On the basis of the above analysis, an intelligent detection method is proposed for activated sludge microorganisms using deep learning. The method initially involves pre-processing, and then feature extraction. Finally, a microbial information analysis module is used to achieve intelligent identification of microorganisms from micrographs of activated sludge. Simultaneously, we construct a dataset comprising 2000 micrographs of activated sludge microorganisms to test the performance of the proposed method and compare it with other detection approaches for activated sludge microorganisms.

The remainder of this study is organized as follows: Section 3 describes the methodology, including the construction of the activated sludge microorganism image dataset and the intelligent detection method for activated sludge microorganisms. Section 4 presents the relevant experiments conducted using the microbial image dataset and the results analysis. The final section summarizes the study and provides the related research conclusions.

3. Methodology

This study involves the creation of a micrograph image dataset comprising activated sludge microorganisms for sewage treatment and the development of an intelligent detection method for these microorganisms, termed the activated sludge microbial detector (ASMDetector), as illustrated in Fig. 1. The intelligent microorganism detection method consists of three stages: pre-processing, feature extraction, and microbial information analysis.

3.1 Construction of activated sludge microorganism micrograph image dataset

A micrograph image dataset of microorganisms was constructed using sewage samples. An appropriate volume of water samples was collected, as depicted in Fig. 2, and micrographs were acquired using an Olympus BX53 optical microscope camera, as shown in Fig. 3.

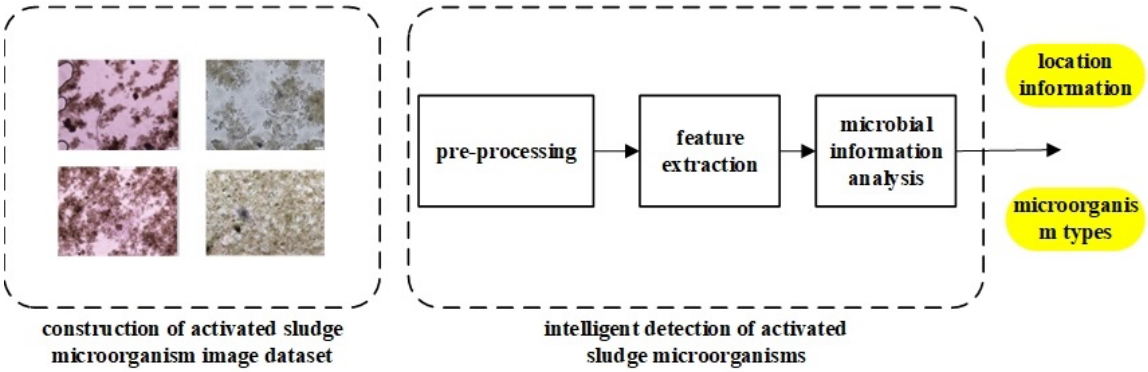

Fig. 1. Schematic illustration of the proposed method

Detection personnel annotated micrographs for four microorganism types: *Epistylis*, *Nematoda*, *Lecane*, and *Arcella*. The abundance of each microorganism is presented in Table 1. Fig. 4 displays partial, zoomed-in images of representative microorganisms from the dataset, magnified at 40×, 100×, and 200×.

Fig. 2. Activated sludge at the end of the sewage aerobic biological treatment tank

Fig. 3. OLYMPUS BX53 optical microscope

Table 1. Activated sludge microorganism micrograph image dataset

microorganism	image quantity	microorganism quantity
Epistylis	500	2718
Nematoda	500	3009
Lecane	500	2829
Arcella	500	3129
total	2000	11685

3.2 Intelligent detection of activated sludge microorganisms

The ASMDetector, an intelligent detection method for activated sludge microorganisms, analyzes micrographs $\boldsymbol{I}$ containing microorganisms $\{(x_i, y_i)\}_{i=1}^{K}$ to identify four distinct species: *Epistylis*, *Nematoda*, *Lecane*, and *Arcella*. As shown in Fig.5, the detection process comprises three stages, namely, pre-processing, feature extraction, and microbial information analysis.

(1) Pre-processing Module: The micrographs of microorganisms are uniformly divided into blocks with specified width $Width_p$ and height $Height_p$. The range for $Width_p$ is [128, $Width/2$], and the range for $Height_p$ is [128, $Height/2$]. Here, Width and Height represent the width and height of the micrographs, respectively.

(2) Feature Extraction Module: This module extracts features from the image blocks to obtain feature maps $F \in F^{h \times w \times c_1}$ (where h, w, and c_1 represent the height, width, and number of feature channels of the feature map, respectively). The feature map F is then input into the microbial information analysis module (MIAM).

(3) Microbial Information Analysis Module (MIAM): Based on the features F from the feature extraction module, the MIAM generates prediction results (types and locations of microorganisms) through the microbial recognition unit and the microbial localization unit.

3.3 Microbial information analysis module

MIAM comprises four key components: the microbial information extraction unit (FIEU), a global information fusion feature extraction unit, a microbial recognition unit,

and a microbial localization unit. The architectural overview is depicted in Fig.6.

(1) FIEU: This unit consists of two multi-layer perceptron (MLP) modules, namely, L high-level feature extraction modules (HLFEM) and L low-level feature extraction modules (LLFEM), where L is a configurable parameter. The specific structure and operational process will be detailed in Section 3.4.

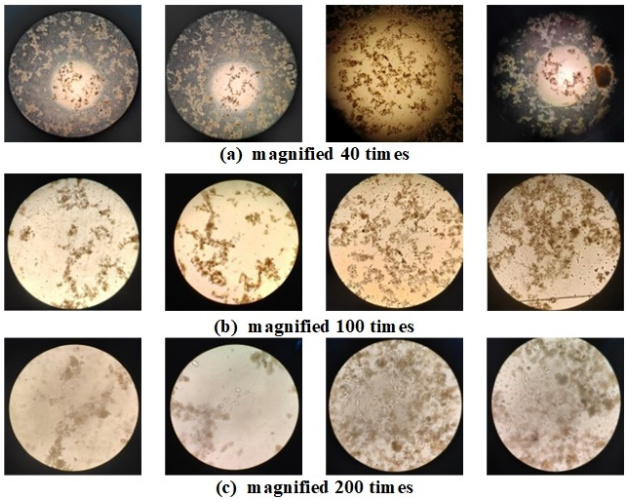

Fig. 4. Partial zoomed-in images of activated sludge microorganisms

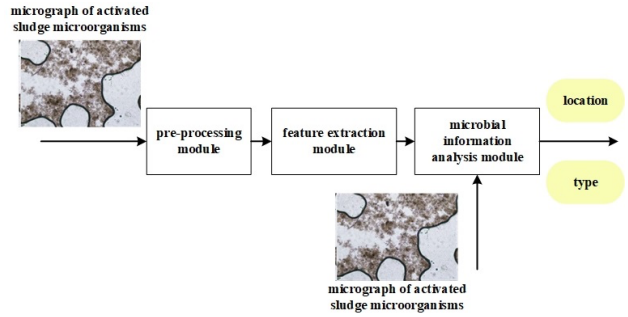

Fig. 5. Intelligent detection process of activated sludge microorganisms

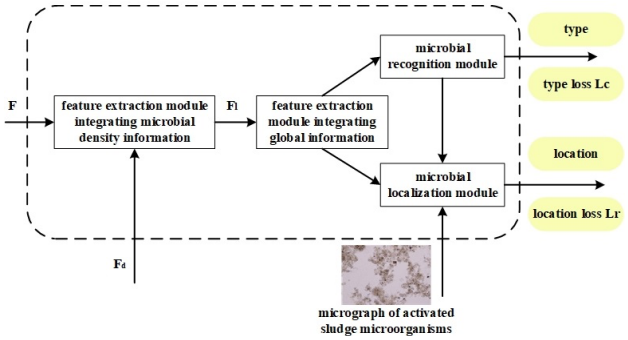

Fig. 6. Structure of the microbial information analysis module

(2) Global Information Fusion Feature Extraction Unit: This unit is responsible for extracting and fusing features from the microorganism image blocks. Its architecture comprises L layers (configurable and consistent with the FIEU configuration), each containing a self-attention module, a cross-attention layer, and a feed-forward network (FFN).

(3) Microbial Recognition Unit: Leveraging input features, this unit generates predicted microorganism types. Its architecture is detailed in Table 2.

Table 2. Structure of the microbial recognition unit

layer	type
1	*Conv(3, 3, 1, 1)*
2	*Conv(3, 3, 1, 1)*
3	*Conv2d(1x1, 1, 0, N_{cls})*

(4) Microbial Localization Unit: This unit predicts the locations of microorganisms by using input features. Its architectural configuration is presented in Table 3.

Table 3. Structure of the microbial localization unit

layer	type
1	*Conv(3, 3, 1, 1)*
2	*Conv(3, 3, 1, 1)*
3	*Conv2d(1x1, 1, 0, 4xreg_max)*

The MIAM operates as follows: The feature map $\boldsymbol{F}$ generated by the feature extraction module, is initially input into the FIEU, producing analysis features $\boldsymbol{F^L}$ for microorganisms. Subsequently, the analysis features $\boldsymbol{F^L}$ and the micrographs of the activated sludge microorganisms are transmitted to the global information fusion feature extraction unit. The integrated information is concurrently forwarded to the microbial recognition unit and the microbial localization unit, yielding predicted microbial information, namely, microorganism types and locations. The FIEU employs a uniquely designed fine network architecture to generate more effective analysis features $\boldsymbol{F^L}$ for microbial information. These features are subsequently mapped to confidence scores via the microbial recognition unit and to point coordinates through the microbial localization unit. Let $\left\{p_i\left(\hat{x}_i,\hat{y}_i\right)\right\}_{i=1}^{n}$ denote the prediction results for all queries, where p_i represents the predicted confidence of the point belonging to the foreground, and $\{(x_i,y_i)\}_{i=1}^{K}$ refer to the predicted coordinates of the *i-th* query. Subsequently, a k-nearest neighbor matching process is conducted between the prediction results $\left\{p_i\left(\hat{x}_i,\hat{y}_i\right)\right\}_{i=1}^{n}$ and the ground truth. Each microorganism, each microorganism $\{(x_i,y_i)\}_{i=1}^{K}$ possesses a corresponding matched prediction result given that n is greater than $\boldsymbol{NUM}$.

The loss function of the microbial information analysis module is contingent upon two primary factors: the confidence associated with the prediction results and the average nearest neighbor distance between the predicted and ground truth data. Consequently, the loss function of the activated sludge microorganism detection network is expressed as follows:

$$L_{MA} = L_c + L_l \tag{1}$$

where L_c denotes the classification loss, which enhance the confidence of matched predictions while suppressing that of unmatched predictions. To localization loss L_l , which quantifies the distance L_l also computed, which quantifies the distance L_l between matched predicted coordinates and their corresponding ground truth coordinates, is also computed to oversee the learning process of the predicted coordinates. The classification loss L_c is computed using Equation (2), where y_i represents the actual class of the microorganism, $\sigma(x_i)$ indicates the predicted class by the model, and $\boldsymbol{n}$ is the number of microorganisms.

$$L_c = -\frac{1}{n}\sum_{i}^{n}\left[y_i * \log\left(\sigma\left(x_i\right)\right) + \left(1-y_i\right) * \log\left(1-\sigma\left(x_i\right)\right)\right] \quad (2)$$

The localization loss L_l employs the intersection over union (IoU) loss function to quantify the overlap between the predicted bounding box and the corresponding ground truth box, thereby evaluating the accuracy of the detected box. The IoU value of each predicted box is computed with respect to all ground truth boxes, which exhibit the maximum IoU designated as its corresponding match. The IoU loss is subsequently calculated using Equation (3), as follows:

$$L_l = 1 - IoU\left(b, b^{gt}\right) + \frac{p^2\left(b, b^{gt}\right)}{c^2} \quad (3)$$

where $p^2\left(b, b^{gt}\right)$ represents the Euclidean distance between the center points of the predicted bounding box $\boldsymbol{b}$ and the ground truth box b^{gt}, $\boldsymbol{c}$ denotes the diagonal length of the image, and $IoU\left(b, b^{gt}\right)$ is the intersection over union ratio between the predicted bounding box $\boldsymbol{b}$ and the ground truth box b^{gt}, calculated using Equation (4), as follows:

$$IoU\left(b, b^{gt}\right) = \frac{\left|b \cap b^{gt}\right|}{\left|b \cup b^{gt}\right|} \quad (4)$$

3.4 Key technology: microbial information extraction unit

The network architecture of the FIEU is depicted in Fig.7. It comprises two MLP modules, HLFEM and LLFEM, where $\boldsymbol{L}$ is a configurable hyperparameter with a range of 3 to 8 and a default value of 4. The input to the FIEU includes the feature map $\boldsymbol{F}$ derived from the feature extraction sub-network.

The operational process of the FIEU is as follows. Initially, an MLP layer maps the feature $\boldsymbol{F}$ to $\hat{F} \in F^{h \times w \times c}$, and another MLP layer maps $\boldsymbol{F}$ to $\hat{F}_d \in R^{h \times w \times c}$ to align the feature channels (c). The input to the first HLFEM module is $\hat{F}$. This process is expressed by the following equation:

$$F^1 = R_s\left(\hat{\mathbf{F}}\right) + R_s\left(\hat{\mathbf{F}}_d\right) + E;\ F^2 = HLFE\left(F^1\right) \quad (5)$$

where $R_s(\bullet)$ denotes the operation of reshaping the feature map by flattening the spatial dimensions, and $HLFE(\bullet)$ represents the HLFE module. Subsequent HLFE modules further refine the features as follows:

$$\begin{aligned} &F_d^1 = F_d, \\ &F_d^i = LLFE\left(F_d^{i-1}\right), i = 2,3...,L-1, \\ &F_d^{i+1} = HLFE\left(F_d^i + R_s\left(F_d^i\right)\right), i = 2,3...,L-1. \end{aligned} \quad (6)$$

where $LLFE(\bullet)$ refers to the LLFE module. The total number of HLFE modules is $\boldsymbol{L}$, which also signifies the total number of times high-level and low-level features are fused. Subsequent to Equation (6), the microbial information analysis features $F^L \in R^{h \times w \times c}$ are acquired and transmitted to the global information fusion feature extraction unit. The operational process of the FIEU can be elucidated from the perspectives of high-level and low-level information. Prior to each HLFE module in Equation (6), the high-level features from the preceding HLFE module and the low-level features from the LLFE module are integrated. This progressive fusion of high-level and low-level features augments the feature representation capacity of the module.

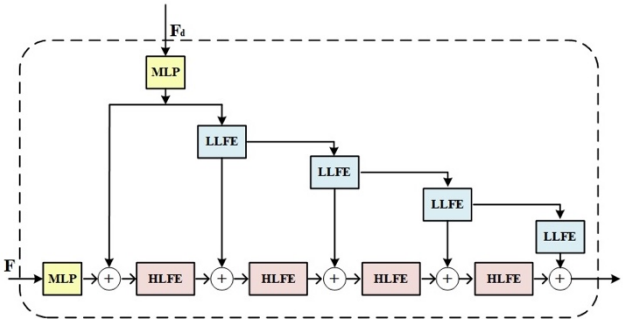

Fig. 7. Network structure of the FIEU (example with L=4)

Table 4. Division of the activated sludge microorganism micrograph image dataset

number of images			microorganism	number of microorganisms			
train	validation	test		total	train	validation	test
350	50	100	*Epistylis*	4718	3217	510	991
			Nematoda	4009	2826	441	742
			Lecane	3827	2577	371	879
			Arcella	3126	2162	363	601
			total	15680	10782	1685	3213

4. Result analysis and discussion

4.1 Comparison methods

Six intelligent detection methods employing diverse technical approaches were selected as benchmarks for evaluating activated sludge microorganism detection performance. These approaches include YOLO v3 [31], YOLO v5 [32], P2PNet [33], CLTR [34], MPS [35], and DSSI-Net [36]. Among these, YOLO v3 and YOLO v5 are classified as recognition-by-detection methods, P2PNet and CLTR as recognition-by-regression methods, and MPS and DSSI-Net as recognition-by-density-generation methods.

4.2 Experimental setup

In the experiments, the activated sludge microorganism image dataset was used for training and testing purposes. Initially, the 500 images containing microorganisms were randomly partitioned into training, validation, and test sets in a 7:1:2 ratio, as outlined in Table 4. Subsequently, data augmentation techniques, including horizontal mirroring,

random jitter, and horizontal offset, were applied to the training set.

For comparative analysis, YOLO v3, YOLO v5, P2PNet, CLTR, MPS, and DSSI-Net were implemented using their respective open-source codes and default parameters. The training configuration of the proposed method is as follows: for the pre-processing module network, the width $Width_p$ and height $Height_p$ of the image blocks were set to 1024 pixels; for the loss function calculation, the tuning value ***NUM-T*** was set to 50. For MIAM and FEIMD, the number of high-level and low-level feature extraction modules ***L*** was set to 4. During training, each batch contained two image blocks (batch size = 2), and the Adam optimizer was used with the number of epochs set to 150. The hardware platform and software environment used for the experiments are shown in Table 5.

Table 5. Hardware and software configuration for the experiment

Hardware	Software
CPU Intel(R) Core i7-8700K	Python 3.9.18
GPU 4 x RTX 2060 12GB	Anaconda 3 2023.09.0
Memory 128 G	CUDA 11.0
/	PyTorch 1.12.1

4.3 Evaluation metrics

The efficacy of the proposed method relative to comparative approaches is evaluated by computing the mean absolute error (MAE) and mean squared error (MSE) between predicted and ground-truth activated sludge microorganism counts derived from image annotations, using Equations (7) and (8). A smaller value of these metrics indicates lower average counting error of the corresponding method, and consequently enhanced performance. y and $\hat{y}$ represent the sets of actual annotations and the predicted microorganism counts using the detection methods in the images, respectively. MRE presents the number of micrographs of activated sludge microorganisms that must be detected, and y_i and $\hat{y}_i$ represent the actual annotated count and the predicted microorganism count in the *i-th* micrograph of activated sludge microorganisms, respectively.

$$MAE\left(y,\hat{y}\right)=\frac{1}{m}\sum_{i=1}^{n}\left|y_i-\hat{y}_i\right| \tag{7}$$

In equation (7), the MAE is also known as the L1 norm loss.

$$MSE\left(y,\hat{y}\right)=\frac{1}{m}\sum_{i=1}^{n}\left(y_i-\hat{y}_i\right)^2 \tag{8}$$

In equation (8), the MSE is also known as the L2 norm loss.

4.4 Comparative experiments on different activated sludge microorganism detection methods

We leveraged the experimental setup detailed in Section 4.2 to compare the performance of various object detection methods on activated sludge microorganisms in micrographs. These methods included YOLO v3 [31], YOLO v5 [32], P2PNet [33], CLTR [34], MPS [35], DSSI-Net [36], and the proposed ASMDetector method. The results are presented in Table 6 and Fig.8 and 9. Table 6 summarizes the MAE and MSE for each method, highlighting the superior performance of ASMDetector using the lowest MAE and MSE values. Fig.8 and 9 visually represent these errors, with the height of the blue rectangles corresponding to the respective MAE (Fig.8) and MSE (Fig.9) values for each method.

Table 6. Comparative results of activated sludge microorganism detection experiments (best results highlighted in bold)

Method	Test(all)	
	MAE	MSE
YOLO v3	17.37	32.36
YOLO v5	9.16	16.69
P2PNet	6.11	12.89
CLTR	6.51	13.52
MPS	8.67	14.87
DSSI-Net	8.44	20.2
ASMDetecor	**5.86**	**12.43**

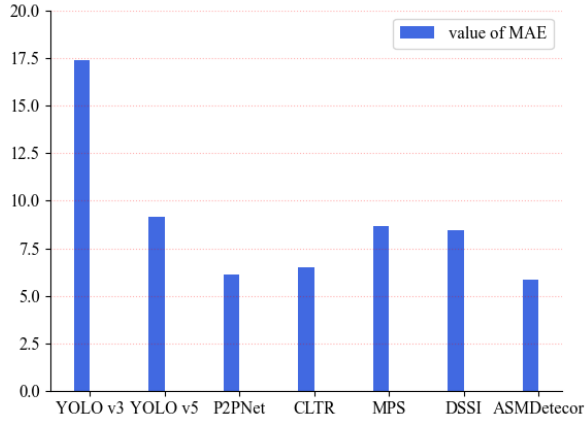

Fig. 8. Performance comparison of different methods for intelligent detection of activated sludge microorganisms (MAE metric)

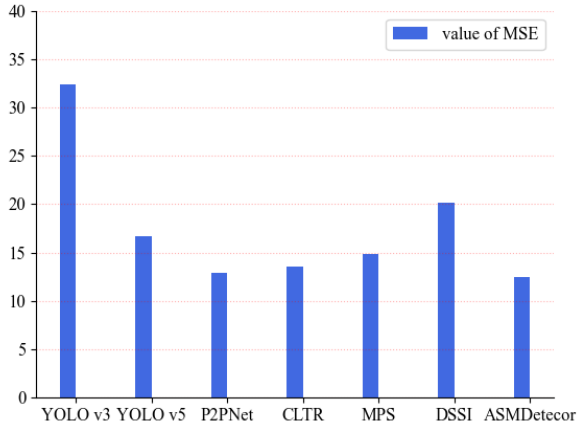

Fig. 9. Performance comparison of different methods for intelligent detection of activated sludge microorganisms (MSE metric)

Table 6 and Fig. 8 and 9 indicate that the proposed method outperforms existing methods ([31]-[36]) in detecting four types of microorganisms across the entire test set, as evidenced by lower MAE and MSE values. While object detection methods, such as YOLO v3 and YOLO v5 exhibit limited performance with dense target identification in complex backgrounds, recognition-by-regression (P2PNet, CLTR) and recognition-by-density-generation (MPS, DSSI-Net) approaches yield better results. However, these methods present room for enhancement in network architecture and processing pipelines. By contrast, the proposed method comprehensively addresses the challenges of activated sludge image analysis by incorporating image pre-processing, feature

extraction, and in-depth feature exploration, followed by microbial information analysis. The comparative experimental outcomes validate the efficacy of the proposed method for accurate microorganism detection within the complex visual context of activated sludge.

4.5 Performance analysis of four types of microorganisms

Table 7 provides a quantitative comparison of the proposed method and six alternative approaches for identifying four activated sludge microorganisms (*Epistylis*, *Nematoda*, *Lecane*, and *Arcella*). Fig.10-13 present bar charts illustrating the performance of each method to facilitate visualization of these results.

Analysis of the MAE and MSE metrics presented in Table 7 and Fig.10-13 demonstrates that the proposed method outperforms comparative approaches in detecting *Epistylis*, *Nematoda*, *Lecane*, and *Acella* microorganisms. These empirical results validate the suitability of the proposed method for activated sludge microorganism detection in real-world sewage disposal contexts. These findings highlight the method's robust generalization capabilities across the four target microorganism types.

Table 7. Comparative results of four microorganism detection experiments (best results highlighted in bold)

Method	Test (*Epistylis*)		Test (*Nematoda*)		Test (*Lecane*)		Test (*Arcella*)	
	MAE	MSE	MAE	MSE	MAE	MSE	MAE	MSE
YOLO v3	5.35	9.91	4.01	7.48	4.76	8.87	3.46	7.18
YOLO v5	2.82	5.14	2.12	3.86	2.51	4.57	1.82	3.36
P2PNet	1.88	3.97	1.41	2.98	1.67	3.53	1.27	2.64
CLTR	2.01	4.16	1.52	3.12	1.81	3.71	1.32	2.73
MPS	2.67	4.58	2.01	3.43	2.38	4.07	1.73	3.02
DSSI-Net	2.59	6.22	1.95	4.67	2.31	5.48	1.71	4.03
ASMDetecor	**1.81**	**3.83**	**1.36**	**2.87**	**1.61**	**3.41**	**1.19**	**2.48**

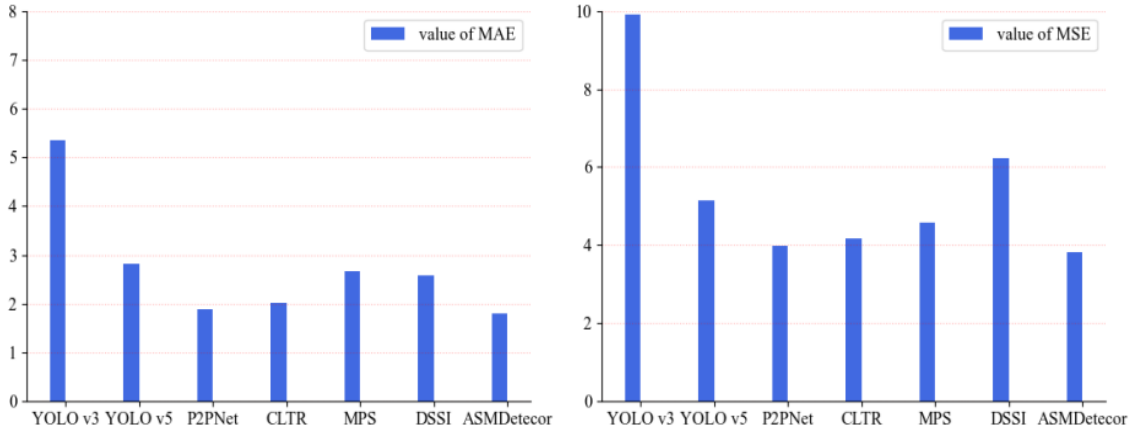

(a) MAE (b) MSE

Fig. 10. Performance comparison of different methods for intelligent detection of *Epistylis*

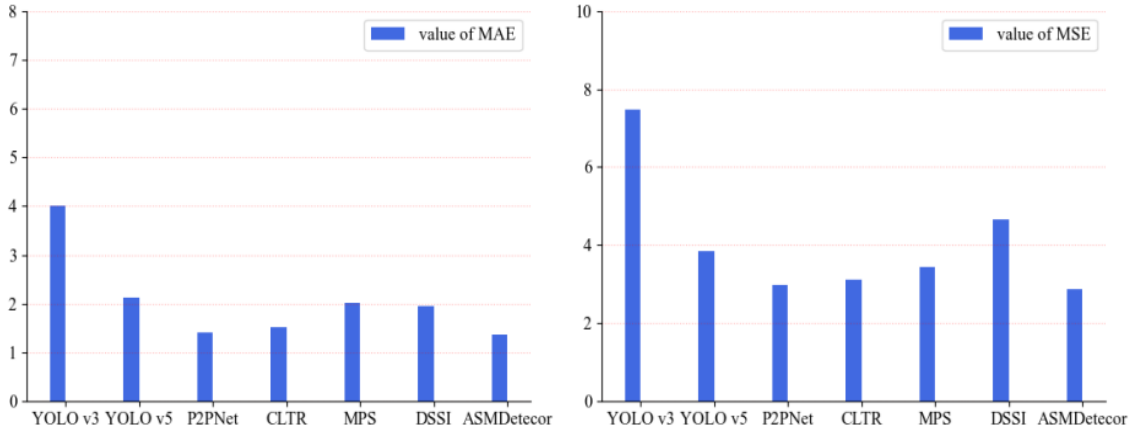

(a) MAE (b) MSE

Fig. 11. Performance comparison of different methods for intelligent detection of *Nematoda*

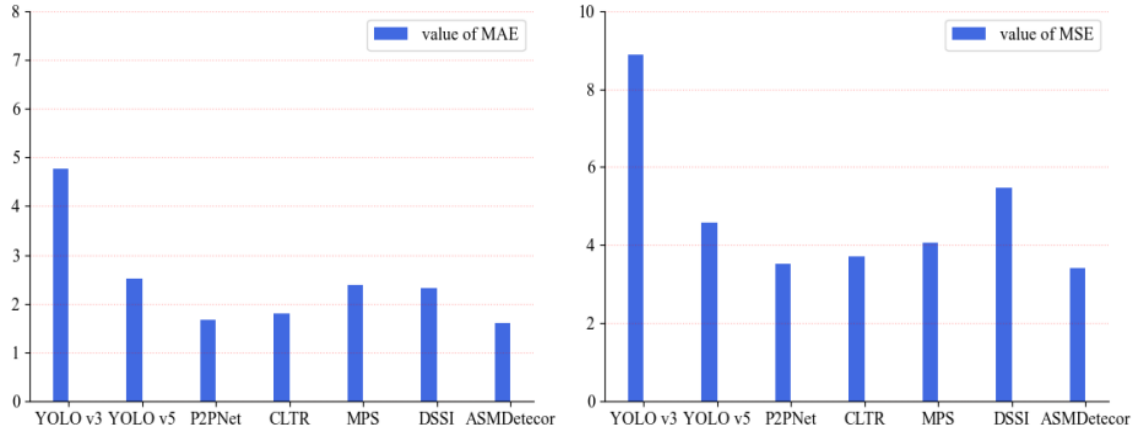

(a) MAE (b) MSE

Fig. 12. Performance comparison of different methods for intelligent detection of *Lecane*

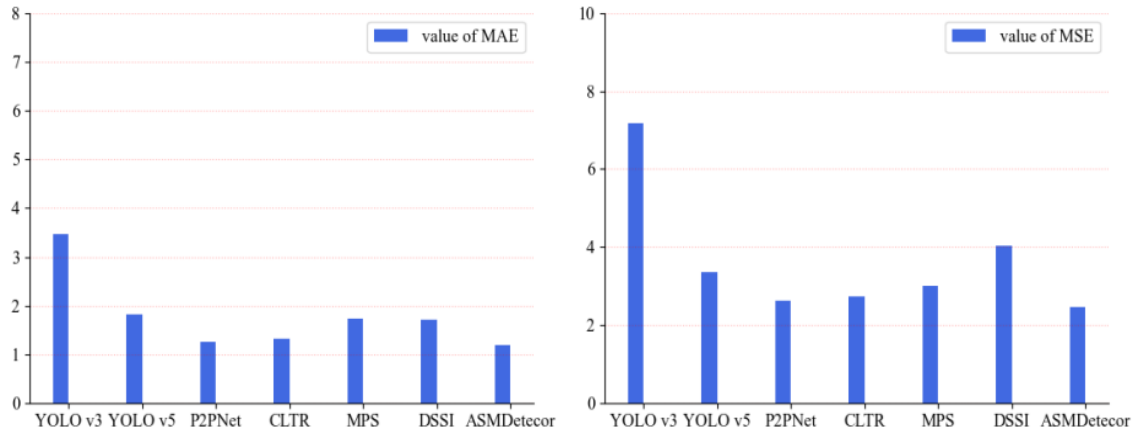

(a) MAE (b) MSE

Fig. 13. Performance comparison of different methods for intelligent detection of *Arcella*

5. Conclusions

This study proposed an intelligent detection method for activated sludge microorganisms based on deep learning. Initially, microbial micrographs underwent pre-processing. Subsequently, a feature extraction module was used to extract microorganism features. Finally, the microbial information analysis module acquired microbial information, encompassing microorganism type and location. To facilitate this study, we constructed an activated sludge microorganism image dataset, meticulously annotated by professional microorganism detection personnel for *Epistylis*, *Nematoda*, *Lecane*, and *Arcella*. Through a comparative analysis of detection results for different microorganism types, we arrived at the following conclusions:

(1) For the task of microorganism detection in activated sludge images from sewage disposal, deep learning methods, with their capacity for automatic image feature discovery, significantly surpass traditional image recognition methods.

(2) Among deep learning methods, recognition-by-density-generation and recognition-by-regression approaches exhibit a performance superior to recognition-by-detection methods. This superiority is evidenced by a reduction in MAE and MSE metrics from 4.26 to 19.93 and 3.3 to 11.51, respectively, in experimental results.

(3) When applying either recognition-by-regression or recognition-by-density-generation methods to activated sludge microorganism detection, factors, such as network architecture, loss functions, and model training strategies significantly influence actual detection performance. By effectively optimizing these factors, our proposed method reduced MAE and MSE metrics by 2.58 to 2.81 and 2.44 to 7.77, respectively, compared with comparative methods.

(4) To effectively evaluate the performance of detection methods, the image dataset employed for training and testing intelligent detection methods for activated sludge microorganisms should accurately reflect the actual characteristics of activated sludge microorganism images. In addition, diverse types of activated sludge microorganisms must be incorporated to assess the generalization capability of detection methods across different microorganism species.

The proposed method successfully achieves intelligent detection of four activated sludge microorganism types: *Epistylis*, *Nematoda*, *Lecane*, and *Arcella*. The proposed method outperforms five existing comparative methods with MAE and MSE metrics of 5.86 and 12.43, respectively, on the test set. This advancement contributes to enhancing the intelligence level of activated sludge microorganism detection and effectively improves the efficiency of water quality monitoring within the sewage disposal process. Nevertheless, further refinements are necessary. Specifically, expanding the image dataset to encompass a broader range of activated sludge microorganisms is crucial for achieving intelligent detection of a wider array of

microorganisms and for augmenting the generalization capability of the detection method.

Acknowledgements

This work was supported by the Scientific Research Projects for College Students of Sichuan University of Arts and Science (No.X2024Z006), the Scientific Research Initiative Program of Sichuan University of Arts and Science (No.2022GCC14Z), the Sichuan University of Arts and Sciences Education Reform Project (No.2023JG057T), the Key Laboratory of Government Data Security (No.ZSAQ202407), the Key Laboratory of Multi-dimensional Data Sensing and Intelligent Information Processing (No.DWSJ2402), and the Sichuan SMT Printing Engineering Technology Research Center (No.SC-SMT-2022-01).

References

[1] J. Pyssa and P. Malek-Palen, "Preliminary studies on the possibility of phosphorus recovery in a sewage treatment plant as an example of the circular economy in the context of biogenic waste," *Przem. Chem.*, vol. 102, no. 11, pp. 1203-1209, Nov. 2023.

[2] M. Sarvajith and Y. V. Nancharaiah, "De novo granulation of sewage-borne microorganisms: A proof of concept on cultivating aerobic granular sludge without activated sludge and effective enhanced biological phosphorus removal," *Environ. Res.*, vol. 224, May. 2023, Art. no. 115500.

[3] Y. Wang, M. Gu, D. Ge, Y. Dong, L. Bai, and N. Zhu, "Polyhexamethylene biguanidine used as a new type sewage sludge conditioning agent: Effect on sludge dewaterability and mechanism," *J. Environ. Manage.*, vol. 315, no. 1, Aug. 2022, Art. no. 115146.

[4] M. Liu, C. Mahata, Z. Wang, S. Kumar, and Y. Zheng, "Comparative exploration of biological treatment of hydrothermal liquefaction wastewater from sewage sludge: Effects of culture, fermentation conditions, and ammonia stripping," *J. Environ. Manage.*, vol. 349, no. 1, Jan., 2024, Art. no. 119527.

[5] R. Hartmann, H. Jeckel, E. Jelli, P. K. Singh, S. Vaidya, and J. C. N. Fong, "Publisher correction: Quantitative image analysis of microbial communities with biofilmQ," *Nat. Microbiol.*, vol. 6, no. 2, pp. 270-286, Feb. 2021.

[6] M. Sobczyk, A. Pajdak-Stós, E. Fiakowska, L. Sobczyk, and J. Fyda, "Multivariate analysis of activated sludge community in full-scale wastewater treatment plants," *Environ. Sci. Pollut. R.,* vol. 28, no. 3, pp. 3579-3589, Jan. 2021.

[7] M. C. G. Reis, A. C. Borges, F. F. D. Cunha, and R. R. D. Silva, "Evapotranspiration beds as a zero-discharge nature-based solution for wastewater disposal: A review," *Ecol. Eng.,* vol. 189, Apr. 2023, Art. no. 106896.

[8] D. Vouk, D. Nakic, A. Bubalo, and T. Bolana, "Environmental aspects in selecting optimum variant of sewage sludge management," *Environ. Eng. Manag. J.*, vol. 21, no. 3, pp. 443-456, Mar. 2022.

[9] Y. N. Zheng, S. Y. Wang, J. H. Guo, H. J. Huang, Z. R. Sun, and Y. Z. Peng, "Trends in the use of protozoan and metazoan in the indication and assessment of WWTP operation," *Microblology.*, vol. 35, no. 12, pp. 1943-1949, Dec. 2008.

[10] Y. Li, Z. Chen, H. L. Li, Q. J. Yao, Y. Wei, and J. S. Jiang, "Improving dewaterability of sewage sludge by inoculating acidified sludge and Fe2+: Performance and mechanisms," *Process. Saf. Environ., Part B*, vol. 158, pp. 210-220, Feb. 2022.

[11] T. Zhou, X. Li, H. Liu, S. M. Dong, Z. H. Zhang, and Q. L. Wang, "Occurrence, fate, and remediation for per-and polyfluoroalkyl substances (PFAS) in sewage sludge: A comprehensive review," *J. Hazard. Mater.*, vol. 466, no. 15, Mar., 2024, Art. no. 106896.

[12] T. R. De, B. B. Rodrigues, S. S. Da, R. A. A. Spinasse, and M. Mestria, "Virtual reality solutions employing artificial intelligence methods: A systematic literature review," *Acm Comput. Surv.,* vol. 55, no. 10, pp. 495-523, Dec. 202.

[13] Z. Jan, F. Ahamed, W. Mayer, N. Patel, G. Grossmann, and A. Kuusk, "Artificial intelligence for industry 4.0: Systematic review of applications, challenges, and opportunities," *Expert. Syst. Appl.*, vol. 216, Apr. 2023, Art. no. 119456.

[14] Y. Liu, Z. Wang, L. H. Peng, Q. Xu, and K. Q. Li, "A detachable and expansible multisensor data fusion model for perception in level 3 autonomous driving system," *IEEE T. Intell. Transp.,* vol. 24, no. 2, pp. 1814-1827, Jun. 2023.

[15] J. H. Guo, W. C. Li, and K. Li, "Model predictive adaptive cruise control of intelligent electric vehicles based on deep reinforcement learning algorithm FWOR driver characteristics," *Int. J. Auto. Tech-Kor.*, vol. 24, no. 4, pp. 1175-1187, Aug. 2023.

[16] L. C. Zhao, H. Zou, X. Xie, D. H. R. Guo, Q. H. Gao, and W. M. Zhang, "Mechanical intelligent wave energy harvesting and self-powered marine environment monitoring," *Nano. Energy.,* vol. 108, Apr. 2023, Art. no. 108222.

[17] M. Soualhi, K. T. P. Nguyen, K. Medjaher, D. Lebel, and D. Cazaban, "Intelligent monitoring of multi-axis robots for online diagnostics of unknown arm deviations," *J. Intell. Manuf.*, vol. 34, no. 4, pp. 1743-1759, Jan. 2023.

[18] M. Yip, S. Salcudean, K. Goldberg, K. Althoefer, A. Menciassi, and C. Lee, "Artificial intelligence meets medical robotics," *Science*, vol. 381, no. 14, pp. 141-146, Jul. 2023.

[19] S. Boussen, J. B. Denis, P. Simeone, L. David, B. Nicolas, and A. M. Univ, "ChatGPT and the stochastic parrot: artificial intelligence in medical research," *Brit. J. Anaesth.*, vol. 131, no. 4, pp. 120-121, Apr. 2023.

[20] Z. Chen, M. Wu, A. Chan, X. L. Li, and Y. S. Ong, "Survey on AI sustainability: emerging trends on learning algorithms and research challenges," *IEEE Comput. Intell. M.*, vol. 18, no. 2, pp. 60-77, Jun. 2023.

[21] M. Shi, H. Lu, C. Feng, H. R. Wang, J. Zhang, and Z. W. Han, "Represent, compare, and learn: A similarity-aware framework for class-agnostic counting," in *Proc. IEEE Conf. Comput. Vis. Pattern Recog.*, New Orleans, LA, USA, 2022, pp. 9519-9528.

[22] C. H. Lai, S. S. Yu, H. Y. Tseng, and M. H. Tsai, "A protozoan parasite extraction scheme for digital microscopic images," *Comput. Med, Imag. Grap.*, vol. 34, no. 2, pp. 122-130, Mar. 2010.

[23] A. L. Amaral, Y. P. Ginoris, A. Nicolau, and E. C. Ferrreria, "Stalked protozoa identification by image analysis and multivariable statistical techniques," *Anal. Bioanal. Chem.*, vol. 391, no. 4, pp. 1321-1325, Jun. 2008.

[24] H. Boztoprak and Y. Özbay, "Detection of protozoa in wastewater using ANN and active contour in image processing," *J. Electr. Eng. Technol.*, vol. 13, no. 2, pp. 1661-1666, Jan. 2013.

[25] D. Kaur, S. Uslu, K. J. Rittichier, and A. Durresi, "Trustworthy artificial intelligence: A review," *ACM Comput. Surv.*, vol. 55, no. 2, pp. 1-38, Jan. 2022.

[26] M. Chignell, L. Wang, A. Zare, and J. Li, "The evolution of HCI and human factors: Integrating human and artificial intelligence," *ACM T. Comput-Hum. Iny.*, vol. 30, no. 2, pp. 1-30, Sep. 2022.

[27] F. Luo, S. Khan, Y. Huang, and K. Wu, "Binarized neural network for edge intelligence of sensor-based human activity recognition," *IEEE T. Mobile. Comput.,* vol. 22, no. 3, pp. 1356-1368, Mar. 2023.

[28] L. Xiao, and Z. M. Lan, "Identification of sewage microorganisms using attention mechanism," *Laser & OE. Prog.*, vol. 60, no. 2, pp. 1-8, Jan. 2023.

[29] Z. H. Wu, "Microbial target detection method in activated sludge micro image," M.S. thesis, Dept. Ctrl. Eng.. Chin., Shenyang Univ. Chem. Tech., Shenyang, China, 2021.

[30] Z. Wang, H. Dai, B. Chen, H. R. Wang, J. Zhang, and Z. W. Han, "Effluent quality prediction of the sewage treatment based on a hybrid neural network model: Comparison and application," *J. Environ. Manage.*, vol. 351, Feb. 2024, Art. no. 119900.

[31] J. Redmon and A. Farhadi. "Yolov3: An incremental improvement." doi.org. Accessed: Feb. 1, 2018. [Online.] Available: https://doi.org/10.48550/arXiv.1804.02767.

[32] G. Jocher. "Yolov5." github.com. Accessed: Feb. 1, 2020. [Online.] Available: https://github.com/ultralytics/yolov5.

[33] Q. Y. Song, C. G. Wang, Z. K. Jiang, Y. B. Wang, Y. Tai, and Y. Wu, "Rethinking counting and localization in crowds: A purely point-based framework," in: *Proc. Int Conf. Comput. Vis.*, Montreal, QC, Canada, 2021, pp. 3345-3354.

[34] D. K. Liang, W. Xu, and X. Bai, "An end-to-end transformer model for crowd localization," in: *Eur. Conf. Comput. Vis.*, Tel Aviv, Israel, 2022, pp. 38-54.

[35] M. Zand, H. Damirchi, A. Farley, M. Mahdiyar, G. Michael, and E. Ali, "Multil-scale crowd counting and localization by multitask point supervision," in: *IEEE Int. Conf. ASSP*, Singapore, Singapore, 2022, pp. 1820-1824.

[36] L. B. Liu, Z. L. Qiu, G. B. Li, S. F. Liu, L. Wan, and L. W. Liang, "Crowd counting with deep structured scale integration network," in: *Proc. Int Conf. Comput. Vis.*, Seoul, Korea (South), 2019, pp. 1774-1783.